Received: 13 September 2024 | Accepted: 2 April 2025

DOI: 10.1111/1365-2435.70051

Functional Ecology

RESEARCH ARTICLE

Climate explains global functional trait variation in bees

Madeleine M. Ostwald[1] | Kathryn Chen[1] | Nicholas Alexander[1] | Luning Ding[1] | Victor H. Gonzalez[2] | Katja C. Seltmann[1]

[1]Cheadle Center for Biodiversity & Ecological Restoration, University of California, Santa Barbara, California, USA

[2]Department of Ecology and Evolutionary Biology, University of Kansas, Lawrence, Kansas, USA

Correspondence
Madeleine M. Ostwald
Email: mostwald@ucsb.edu

Funding information
Division of Biological Infrastructure, Grant/Award Number: 2101851 and 2102006

Handling Editor: Katie Marshall

Abstract

1. Climate is a fundamental driver of macroecological patterns in functional trait variation. However, many of the traits that have outsized effects on thermal performance are complex, multi-dimensional, and challenging to quantify at scale.
2. To overcome this challenge, we leveraged techniques in deep learning and computer vision to quantify hair coverage and lightness of bees, using images of a diverse and widely distributed sample of museum specimens.
3. We demonstrate that climate shapes variation in these traits at a global scale, with bee lightness increasing with maximum environmental temperatures (thermal melanism hypothesis) and decreasing with annual precipitation (Gloger's Rule).
4. We found that deserts are hotspots for bees covered in light-coloured hairs, adaptations that may mitigate heat stress and represent convergent evolution with other desert organisms.
5. These results support major ecogeographical rules in functional trait variation and emphasize the role of climate in shaping bee phenotypic diversity.

KEYWORDS
Bogert's rule, coloration, computer vision, Gloger's rule, insects, lightness, pilosity, thermal melanism hypothesis

1 | INTRODUCTION

Climate drives macroecological patterns in species distributions, abundance, and diversity (Brown, 1995; MacArthur, 1972; Whittaker et al., 2001). A tractable approach for understanding these patterns is by investigating the species traits that mediate organisms' fitness and performance under varying climate conditions (Gagic et al., 2015; Mcgill et al., 2006; Violle et al., 2007). These traits (e.g. body size, coloration, etc.) mediate functional interactions between organisms and their environments, and offer avenues for synthesizing organismal responses with broader-scale biogeographic trends (Mcgill et al., 2006; Violle et al., 2007, 2014). However, whether functional relationships between traits and climate give rise to generalizable patterns at global scales remains a major question in evolutionary ecology (Gaston et al., 2008; He et al., 2023).

For ectotherms, the physical characteristics of the body surface mediate heat exchange with the environment (Angilletta, 2009; Buxton et al., 2021). Variation in body coloration—specifically, colour lightness—influences the absorption of solar radiation, and so represents one mechanism for thermal adaptation (Clusella Trullas et al., 2007; Watt, 1968). Indeed, variation in colour lightness can track environmental gradients. Across taxa, darker coloration has been associated with cooler climates, such as high elevation or high latitude environments (Bishop et al., 2016; Clusella Trullas et al., 2007; Kang et al., 2021; Munjal et al., 1997; Watt, 1968), where it may confer fitness benefits by enabling individuals to

reach operating temperatures more quickly (i.e. the thermal melanism hypothesis or Bogert's Rule, (Bogert, 1949; Clusella Trullas et al., 2007)). Simultaneously, darker individuals may be found in wetter environments, through a variety of proposed mechanisms related to the ecological and physiological functions of melanin (i.e. Gloger's Rule, Delhey, 2019; Gloger, 1833; Lopez et al., 2021; Nishikawa et al., 2010; Rensch, 1929).

Another morphological trait implicated in thermoregulation is pilosity (i.e. hairiness), which can increase boundary layer resistance to convective heat loss (Buxton et al., 2021; Casey & Hegel, 1981; Church, 1960; Heinrich, 1974). Correspondingly, in some taxa, hair length increases with elevation (Gonzalez et al., 2022; Osorio-Canadas et al., 2022; Peters et al., 2016) and latitude (Peat et al., 2005), consistent with its function as insulation. At the same time, the quantity and distribution of hair also influence an organism's reflectance, particularly when the reflective properties of hair contrast with those of the underlying body surface. In this way, light-coloured (i.e. high reflectance) hairs serve a photoprotective function in some heat-adapted plants and insects (Barrett & O'Donnell, 2023; Ehleringer et al., 1976; Mershon et al., 2015; Shi et al., 2015; Skelton et al., 2012). These findings support mechanistic links between lightness, pilosity, and climate, yet, evidence that these traits vary predictably with climate at global scales has remained elusive for most taxa.

A major obstacle to attaining these macroecological insights is the time-demanding nature of trait measurement and data standardization. As a consequence, our understanding of climate–trait relationships is dominated by the traits that are simplest to measure (e.g. body size, see Blackburn & Gaston, 1994; Chown & Gaston, 2010). By contrast, heterogeneous and geometrically complex traits like lightness and especially pilosity are poorly represented in large datasets, despite their importance for thermal performance (Ostwald et al., 2023). Contemporary advances in artificial intelligence (AI) present exciting opportunities to overcome these quantification challenges. Computer vision, a branch of AI that applies machine learning to derive high-dimensional data from images, offers tractable solutions for scalable, automated trait data collection. These techniques are increasingly accelerating ecological data collection, taking advantage of the recent proliferation of image datasets in biological research (Gharaee et al., 2025; Lürig et al., 2021; Seltmann et al., 2021; Van Horn et al., 2018; Weinstein, 2018). In addition to providing pathways to study complex, lesser-studied traits, these tools enable high-throughput trait data collection that extends the scales at which we can test ecological hypotheses.

Here, we develop and apply a computer vision methodology for investigating functional trait variation in bees (Apoidea: Anthophila), the most important animal pollinators of wild and cultivated plants (Ollerton et al., 2011). Bees are diverse and globally distributed, representing over 20,000 described species worldwide and occupying all major terrestrial biomes (Michener, 2007). Likewise, bees are morphologically diverse, spanning a broad range of colour phenotypes and ranging from hairless to thickly pilose. We trained convolutional neural networks (CNNs) to perform feature extraction on images of bees, and used these data to automate the measurement of colour lightness and pilosity across a large, taxonomically diverse bee image dataset. Using these data, we ask the following questions: (i) how does climate shape interspecific variation in bee lightness (i.e. Bogert's Rule and Gloger's Rule)? (ii) how does climate shape interspecific variation in bee pilosity? and (iii) how do these two traits interact? These findings illuminate how climate shapes species assemblages and drives trait diversification at macroecological scales.

2 | MATERIALS AND METHODS

2.1 | Image datasets

For both model training and trait analysis, we used high-resolution, bright-field DSLR macro photographs of preserved bee specimens. All images represent lateral habitus views of the specimens. The lateral view allowed for greater consistency in the viewable portion of the bees' body; in dorsal images, by contrast, the proportion of the body in view is strongly dependent on the relative positions of the mesosoma and metasoma. All specimens were dried and none were stored in preservative (e.g. ethanol).

We trained our models on a total of 230 unique bee images (and associated augmented images, see 'Segmentation model training'), then applied the trained models to a novel set of 611 bee images. We produced the majority of these images (67.5%) by photographing specimens from the University of Kansas Entomology Collections and the University of California, Santa Barbara Invertebrate Zoology Collection using a Canon EOS 6D Mark II camera with a 65 mm lens, StackShot macro-rail (Macroscopic Solutions, East Hartford, CT, USA), and focus stacking using Zerene Stacker. These images are publicly available (Ostwald et al. 2024; Seltmann et al., 2021). We supplemented these images with public domain images captured using the same imaging methodology, from two sources: Exotic Bee ID (Burrows, 2021) (used in model training, $N = 161$ images) and the USGS Native Bee Inventory and Monitoring Program (USGS Interagency Bee Lab, USGS Native Bee Inventory and Monitoring Program Images, 2010; used in trait analysis, $N = 132$ images). To train models that could generalize well to a variety of lateral habitus images, we used a broad sample of 230 images that included male and female bees across six families (Andrenidae: $N = 7$; Apidae $N = 41$; Colletidae: $N = 17$; Halictidae $N = 7$; Megachilidae: $N = 151$; Apidae $N = 7$), specimens with and without visible pins, and images with backgrounds that were either grey or black.

After training, for trait analysis using the trained models, we used a more uniform image dataset consisting of only female bees and only images with black backgrounds ($N = 623$; all taken at the University of Kansas with a single camera/lighting set-up). Female bees and black background images are also well represented in the training dataset. The trait analysis images represent 611 bee species and 377 genera (63% of recognized bee genera) across all seven bee families. Specimens were collected between 1907 and 2019 (mean

collection year = 1972). All images and metadata are available at https://doi.org/10.5281/zenodo.12572898.

2.2 | Segmentation model training

To quantify bee pilosity and lightness, we trained a semantic segmentation model for pixel-by-pixel classification of relevant features (focal body region, hair) from images of bees (Figure 1). Our chosen segmentation model, TernausNet, is a variant of UNet, a widely-used convolutional neural network that has been successfully implemented for biomedical image segmentation (Huang et al., 2020; Ronneberger et al., 2015). TernausNet uses VGG11 architecture, which is pre-trained on a large and diverse labelled image dataset (ImageNet; Iglovikov & Shvets, 2018). We trained models to perform two distinct segmentation tasks: segmentation of the focal region of the bee's body and segmentation of hair (Figure 1). First, the model identifies the bee in the image and segments it from the background, simultaneously removing the specimen pin (if present), eyes, wings, antennae, stinger (hereafter, we refer to the remaining segment of the bee as the 'focal body region'). While eyes, wings, and tongues may contain small hairs, they contribute minimally to the overall pilosity of the bee, and so were removed from our focal body segment. Moreover, including these regions could bias our measurement of hair coverage (% body surface covered in hair) depending on factors such as the visibility of the tongue or the orientation of the wings, which can alternately represent a large or small area of the image. Likewise, inclusion of wings would skew our estimation of lightness due to variation in reflected light depending on wing position. Next, the model takes the output of the first segmentation task (the focal body region) and further segments pixels into 'hair' and 'non-hair' components.

To accomplish these segmentation tasks, we trained two models, one for hair segmentation and one for focal body region segmentation. The training datasets included ground-truth image masks manually created in Adobe Photoshop (Figure 1). Prior to training, we resized training images to 256×256 pixels and converted them to PyTorch tensors, a data structure compatible with our deep learning framework. We also performed colour normalization to better align our data with the TernausNet pretraining dataset (ImageNet) and facilitate the model's ability to learn from the training data. For focal body region segmentation, we divided our dataset of 230 images and associated ground-truth masks into three subsets with a 60:20:20 split for training, testing, and validation (138, 46, and 46 images, respectively). We trained this model over 100 epochs (batch size = 2) then performed an additional round of training to fine-tune the model using an expanded dataset that included the original images as well as two corresponding sets of augmented images, that is, one image that had been flipped (both vertically and horizontally) and one that had been rotated. For hair segmentation, we used a dataset of 441 cropped images of bees and associated hair masks, similarly split into training, testing, and validation subsets with a 60:20:20 split (265, 88, and 88 images, respectively). This model was also trained over 100 epochs (batch size = 2). Due to the time-intensive nature

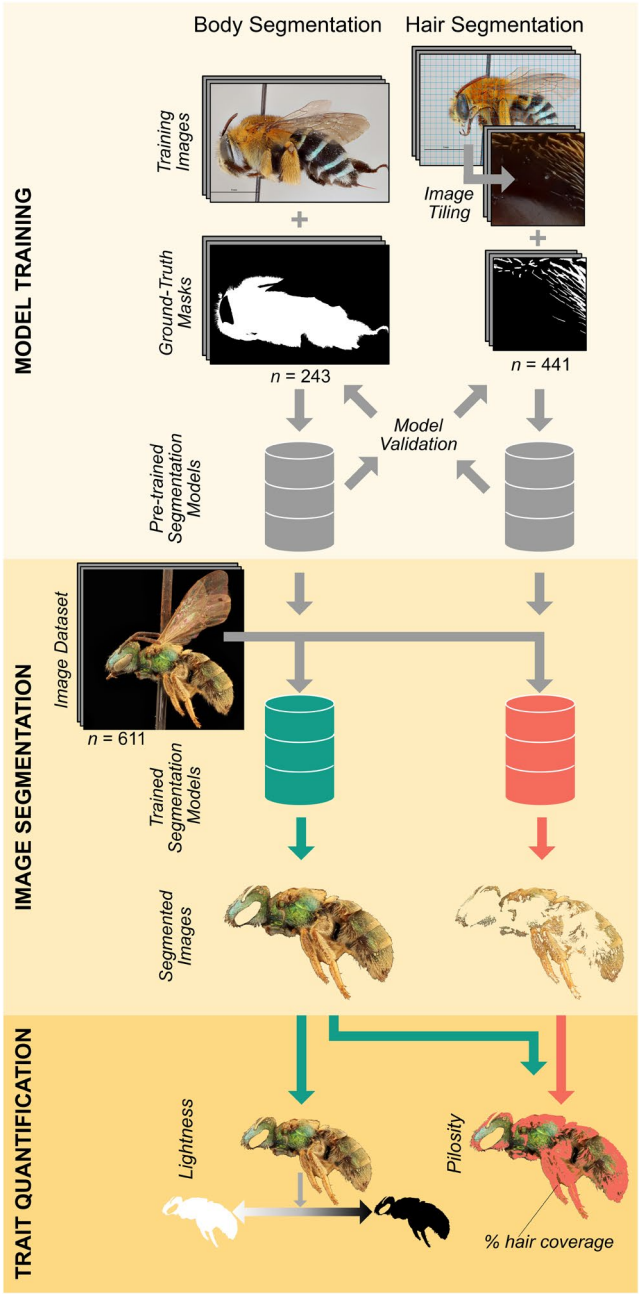

FIGURE 1 Summarized computer vision workflow for feature extraction from images of bees. We trained two CNNs, one for segmentation of the focal body region and one for segmentation of hair. The segmented images from each model are then used to quantify bee lightness and pilosity. Bee lightness is computed as the median pixel lightness value from the focal body region segment. Pilosity is estimated as percent hair coverage, computed by dividing the number of pixels in the hair segment by the total number of pixels in the focal body region segment.

of creating hair masks from images of whole bees, we used image tiling to train the hair segmentation model: we divided input images (mean dimensions: 4269×2975 pixels) into smaller 300×300-pixel crops, then created ground-truth hair masks from randomly chosen cropped images (Figure 1). These crops were then downscaled to 256×256-pixel crops to fit training requirements. This image tiling

procedure is repeated during analysis: prior to hair segmentation, input images are divided into 300×300 pixel crops. The model then segments hair from the cropped images. We then reassemble these segmented crops to reproduce the original full image and calculate a hair coverage score for the entire bee. In this way, the model is able to perform segmentation at the same scale on which it was trained (Figure 1). For all training, we used an Adam optimizer (Kingma & Ba, 2017) and a weighted combination of generalized dice loss and binary cross-entropy loss, with weights of 0.75 and 0.25, respectively (De Boer et al., 2005). Models were implemented in Python 3.9.13. Model training, evaluation, and implementation scripts are available at: https://zenodo.org/doi/10.5281/zenodo.12572908.

We divided our training image dataset into three subsets with a 60:20:20 split for training, testing, and validation, respectively. To evaluate model performance, we report pixel-wise accuracy, *F*1 scores, and intersection over union (IoU) as follows:

$$\text{Pixel} - \text{wise accuracy} = \frac{\text{number of correctly classified pixels}}{\text{total number of pixels}} \times 100\,\%$$

$$F1 = 2\,\text{x}\,\frac{\text{precision} \times \text{recall}}{\text{precision} + \text{recall}}, \text{where}$$

$$\text{precision} = \frac{\text{true positives}}{\text{true positives} + \text{false positives}}, \text{and recall} = \frac{\text{true positives}}{\text{true positives} + \text{false negatives}}$$

$$\text{IoU} = \frac{\text{area of overlap between ground truth mask and predicted mask}}{\text{area of union between ground truth mask and predicted mask}}$$

2.3 | Trait quantification

We quantified pilosity as hair coverage, that is, the percent of the focal body region covered in hair:

$$\%\,\text{hair coverage} = \frac{\text{total segmented hair pixels}}{\text{total segmented focal body region pixels}} \times 100\,\%$$

We measured the lightness of each pixel in the focal body region as a score ranging from 0 (full black) to 255 (full white). To standardize for variation in lighting across images, we calibrated our scores such that the black of the background was set equal to 0. We then computed a lightness score for each pixel in the focal body region and calculated the median lightness across these pixels.

2.4 | Statistical analysis of trait and climate data

To understand relationships between climate variables and trait variation, we fit generalized linear mixed-effects models (GLMM) using the 'lme4' package (Bates et al., 2015) in R version 4.4.2 (R Core Team, 2024). Models were fit with either pilosity or lightness as the response variable and with climate variables as predictors. To account for phylogenetic non-independence of trait values, we included a nested random effect of taxonomic identity (subfamily/genus) (da Silva et al., 2023; Lenoir et al., 2020; Sunday et al., 2011) and used Akaike's Information Criterion (AIC) to confirm that the inclusion of this random effect improved model fit.

We extracted climate data from WorldClim version 2.1 (historical climate data for 1970–2000) at 30 s spatial resolution (~1 km^2); (Fick & Hijmans, 2017) using the 'raster' package (Hijmans, 2023). We associated climate data with the sampling locations of each specimen. Because hair and lightness patterns can vary across a species' range (LaBerge, 1956; Peat et al., 2005), we considered only the climate in the location where a given individual was sampled, rather than the entire range of the species. Where sampling coordinates were not available, we estimated sampling latitude and longitude from the most specific available location data (county, city, or locality) using the geocode() function in the R package 'ggmap' (Kahle & Wickham, 2013). We used these data to describe eight climate variables: (Brown, 1995) mean annual temperature, (MacArthur, 1972) annual precipitation, (Whittaker et al., 2001) temperature seasonality (std. dev. of monthly mean temperatures×100), (Gagic et al., 2015) precipitation seasonality (std. dev of monthly precipitation values×10), (Mcgill et al., 2006) the maximum temperature of the hottest month, (Violle et al., 2007) the minimum temperature of the coldest month, (Violle et al., 2014) the vapour pressure deficit, and (Gaston et al., 2008) solar radiation. These eight variables reflect various measures of the magnitude and variation in environmental moisture and temperature, and were chosen based on predicted relationships between our focal traits and heat and/or water balance (Angilletta, 2009; Barrett & O'Donnell, 2023; Hadley, 1994; Kevan et al., 1982; Shi et al., 2015). We used stepwise backward model selection to identify climate variables associated with pilosity and lightness. We sequentially removed variables based on variance inflation factor to account for collinearity of climate variables (VIF > 5 is a standard threshold; (Rogerson, 2001)), then by removing non-significant variables (type III ANOVA) until we achieved the best-fitting model (lowest AIC). To prevent bias in model selection caused by the order of variable removal, we initially assessed each environmental variable individually (GLMM) to prioritize retention of influential variables in cases where multiple variables had VIF > 5 or $p > 0.05$ (as in Kellermann et al., 2018). We assessed normality of predictor (environmental) and response (trait) variables by inspecting QQ-plots and transformed variables where necessary to improve normality (log-transform: precipitation seasonality; square-root transform: lightness, temperature seasonality, annual precipitation). We confirmed that chosen models met assumptions of GLMM by inspecting QQ-plots of residuals and plots of fitted values versus residuals.

To understand whether biome predicts trait variation, we similarly fit GLMMs with trait values (pilosity or lightness) as response variables, biome as a predictor variable, and nested taxonomic classification (Subfamily/Genus) as a random effect. We used a simplified version of the World Wildlife Fund's terrestrial ecoregions delineation scheme to assign specimens to one of four merged biome categories: (Brown, 1995) Tropical and Subtropical Forests (WWF biomes 1, 2, and 3), (MacArthur, 1972) Temperate Forests (WWF biomes 4, 5, and 12), (Whittaker et al., 2001) Grasslands and Shrublands (WWF biomes 7, 8, 9, and 10), and (Gagic et al., 2015)

Deserts & Xeric Shrublands (WWF biome 13); (Olson et al., 2001). We excluded from our analysis specimens collected in WWF biomes 6, 11, and 14 (Boreal Forests/Taiga, Tundra, Mangroves), due to low sample size from these regions. Similar to the above analyses, we used diagnostic plots to verify that model residuals met assumptions of normality and homoscedasticity, and confirmed that the random effect improved model fit by comparing AIC values. Finally, we used the estimated marginal means ('emmeans' package, (Lenth, 2021)) to calculate *p*-values for pairwise comparisons among the different biome categories.

To understand the extent to which different taxonomic levels explained variation in pilosity and lightness, we fit mixed models for each trait with genus, subfamily, and family identity as nested random effects. We then used variance component analysis to estimate the amount of variation in trait values explained by each taxonomic level ('lme4' package, Bates et al., 2015).

To estimate phylogenetic signal in bee pilosity and lightness, we used a recent genus-level supermatrix phylogeny of the Anthophila (Henríquez-Piskulich et al., 2024). A subset of genera in our dataset was not represented in this tree, so we added them manually to the tree as polytomies with the most closely related genus, based on published phylogenies for each taxon (Bossert et al., 2022; Freitas et al., 2023; Gonçalves, 2016; Gonzalez et al., 2012, 2017, 2019; Litman et al., 2013; Michez et al., 2009; Pisanty et al., 2022; Rasmussen & Cameron, 2009). We calculated mean trait values for each genus, then used the 'phytools' package to estimate phylogenetic signal in pilosity and lightness as Pagel's λ, a scaling parameter that ranges from $\lambda=0$ (no correlation between species) to $\lambda=1$ (strong correlation between species, equal to that expected under a Brownian Motion model of trait evolution; Revell, 2024). We visualized mean trait values across this phylogeny using the 'ggtree' package (Guangchuang et al., 2017).

Finally, we assessed phylogenetic independent contrasts (PIC) to describe the relationship between pilosity and lightness while accounting for phylogenetic non-independence, using the 'ape' package (Paradis & Schliep, 2019).

3 | RESULTS

3.1 | Segmentation model performance

Our models showed high performance in segmentation tasks across a diversity of bee taxa. For focal body region segmentation, pixel-wise accuracy was 98.479 ± 2.746% (mean ± SD), an F1 score of 0.960 ± 0.050, and an IoU score of 0.926 ± 0.0573. Segmentation was performed accurately across bee families despite overrepresentation of certain families in our training dataset (mean accuracy >95% for each family). Indeed, there was no correlation between mean family-level accuracy and the number of training images for that family (Spearman's rank correlation test: $p=0.774$), suggesting that the learned features that are useful for body segmentation are shared across bees and not specific to families. Hair segmentation likewise was performed with high accuracy (accuracy = 86.739 ± 1.442%), though other performance metrics were lower than for body segmentation ($F1=0.593\pm0.039$, IoU = 0.482 ± 0.037). Importantly, predicted hair coverage was strongly correlated with hair coverage in ground-truth masks (Pearson's $r=0.631$, $p<0.001$), suggesting that despite some segmentation limitations, our model captures meaningful variation in hair coverage across bee taxa.

3.2 | Phylogenetic patterns in bee functional trait variation

The output of our computer vision workflow (Figure 1) revealed dramatic variation in pilosity and lightness across bee species. We quantified pilosity as the percent of the body surface covered in hair (mean bee hair coverage = 44.02%; SD = 17.25%; range = 4.59 to 88.87%), and lightness as the median pixel lightness across the bee's body, according to the HSL (Hue-Saturation-Lightness) colour model, where the lightness component ranges from 0 (full black) to 255 (full white); (mean bee lightness = 73.80; SD = 24.10; range = 20 to 168). Pilosity was significantly, positively associated with lightness, with hairier bees being overall lighter in colour (phylogenetic independent contrasts: $\beta=0.658$, $R^2=0.843$, $p<0.001$; Figure 2). We detected significant, moderate phylogenetic signal in both pilosity (likelihood ratio test: $p<0.001$, $\lambda=0.694$) and lightness (likelihood ratio test: $p<0.001$, $\lambda=0.752$). Genus-level differences explained much of the variation in trait values (variance components analysis: $\text{pilosity}_{\text{genus}}=44.2\%$ of total variance, $\text{lightness}_{\text{genus}}=38.3\%$ of total variance), while differences at the level of subfamily and family were less explanatory of trait variation (variance components analysis: $\text{pilosity}_{\text{subfamily}}=5.7\%$; $\text{pilosity}_{\text{family}}=5.9\%$; $\text{lightness}_{\text{subfamily}}=9.7\%$; $\text{lightness}_{\text{family}}=6.1\%$ of total variance). In other words, the diversity of trait phenotypes was well represented within each major family (Figure 2). High residual variance ($\text{pilosity}_{\text{residual}}=44.2\%$; $\text{lightness}_{\text{residual}}=45.9\%$ of total variance) suggests that trait variation is only partially explained by taxonomic level, highlighting the potential importance of other factors, including environmental variation.

3.3 | Climatic and biogeographic patterns in bee pilosity and lightness

To understand how climate shapes functional trait variation, we linked trait to climate data estimated from specimen collection location. The best-fitting models exploring these trait-climate relationships highlighted temperature and precipitation as important drivers of trait variation, while accounting for phylogenetic effects. Specifically, high temperatures (the maximum temperature of the hottest month) significantly predicted variation in both traits (GLMM: $R^2_{\text{c,pilosity}}=0.530$; $R^2_{\text{m,pilosity}}=0.020$; $R^2_{\text{c,lightness}}=0.484$; $R^2_{\text{m,lightness}}=0.038$), with hairier, lighter-coloured bees found in regions with hotter maximum temperatures (ANOVA: $p_{\text{pilosity}}<0.001$;

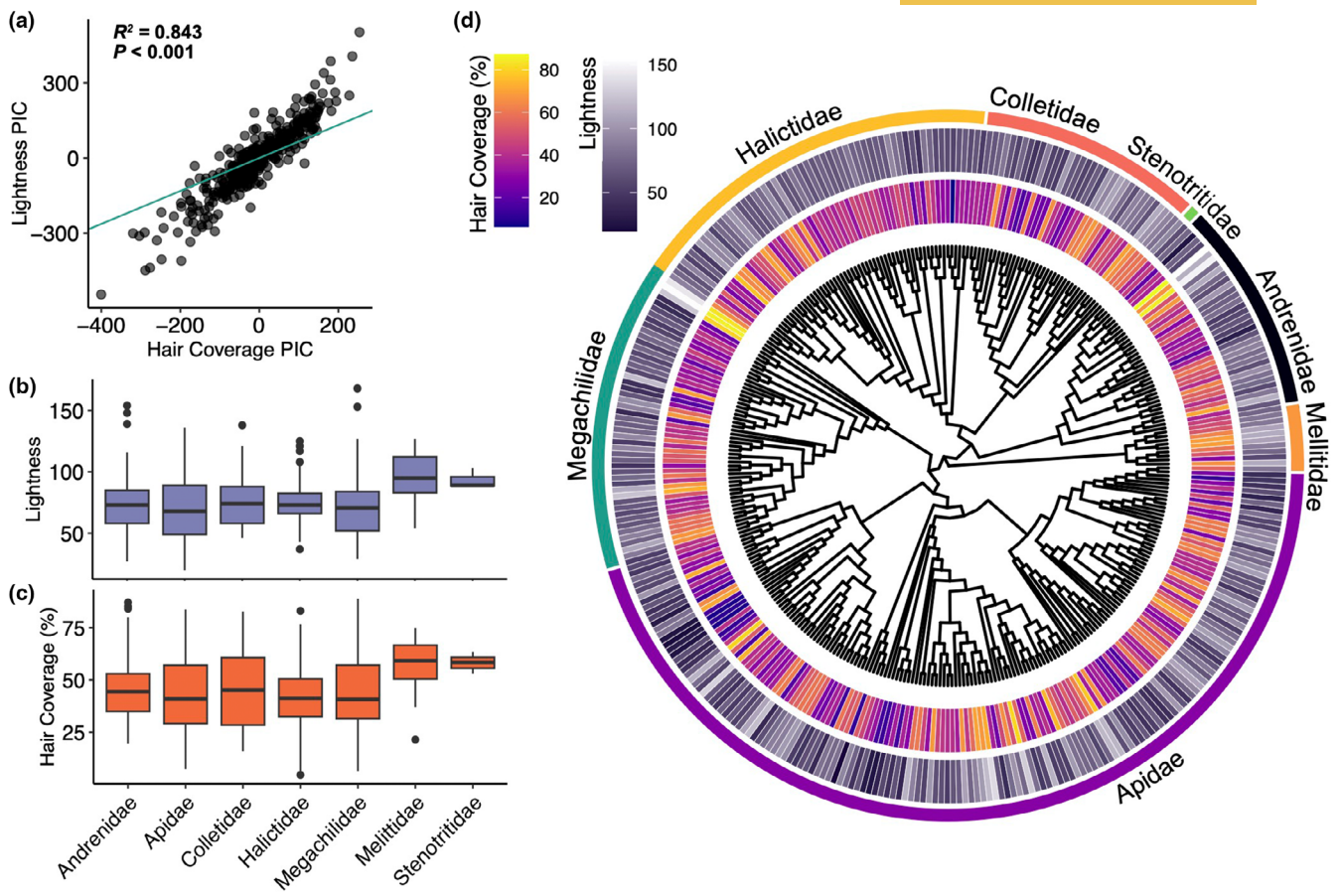

FIGURE 2 Interspecific variation in pilosity and lightness across the bee phylogeny (b–d). Tree tips represent genera, and colours indicate genus-level mean trait values (d). Pilosity values represent percent hair coverage from 0% to 100%. Lightness values represent median lightness values of all bee pixels on a scale from 0 (full black) to 255 (full white). (a) Pilosity and lightness are positively associated (phylogenetic independent contrasts: $\beta = 0.658$, $R^2 = 0.843$, $p < 0.001$).

$\beta_{pilosity} = 0.580$; $p_{lightness} < 0.001$; $\beta_{lightness} = 0.045$; Figure 3). Annual precipitation (square-root transformed) also predicted variation in bee lightness (GLMM: $R^2_{c,lightness} = 0.484$; $R^2_{m,lightness} = 0.038$), with lighter bees found in drier climates (ANOVA: $p_{lightness} = 0.008$; $\beta_{lightness} = -0.014$; Figure 3). Correspondingly, biome significantly predicted bee pilosity and lightness (GLMM: $p_{pilosity} < 0.001$; $p_{lightness} = 0.007$; $R^2_{c,pilosity} = 0.545$; $R^2_{m,pilosity} = 0.027$; $R^2_{c,lightness} = 0.523$; $R^2_{m,lightness} = 0.039$). Bees collected in deserts and xeric shrublands were significantly hairier and lighter-coloured than bees found in the other biomes sampled (temperate forests, tropical and subtropical forests, grasslands and shrublands; $p_{pilosity} < 0.01$ and $p_{lightness} < 0.01$ for all pairwise comparisons to desert; $p > 0.05$ for all other comparisons; Figures 4 and 5).

4 | DISCUSSION

Our study provides evidence for the role of climate in shaping interspecific variation in bee functional traits at a global scale. By leveraging advances in deep learning and computer vision, we generated a large trait dataset with broad geographic coverage representing over 600 species from more than 60% of described bee genera. Our analysis demonstrates that hot, dry regions of the world are hotspots for bees with adaptations that may reduce overheating, namely, coverage with light-coloured hair (Barrett & O'Donnell, 2023; Ehleringer et al., 1976; Mershon et al., 2015; Shi et al., 2015; Skelton et al., 2012). These findings implicate climate factors in bee trait evolution and emphasize the utility of deep learning and computer vision for expanding the scope of functional trait research.

We found that bee hair coverage and lightness both increase with maximum environmental temperature. These patterns may reflect an adaptive thermoregulatory function of light-coloured hair, which has been shown in plants and other insects to mitigate heat stress by increasing reflectance (Barrett & O'Donnell, 2023; Ehleringer et al., 1976; Mershon et al., 2015; Shi et al., 2015; Skelton et al., 2012). Indeed, we detected a strong correlation between these two traits, indicating that hairier bees were lighter coloured. Bee hairs tend to be lighter in colour than the underlying integument, which is often dark (with notable exceptions of dark-haired bees, such as many *Bombus* species, and bees with light integument, for example, many stingless and Anthidiine bees). These findings are consistent with the thermal melanism hypothesis, which posits that

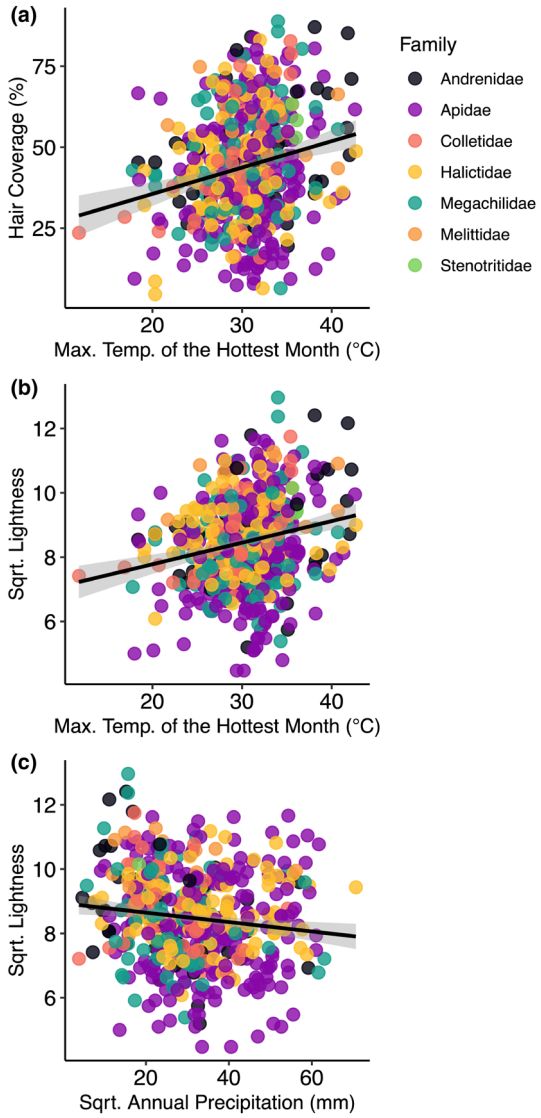

FIGURE 3 Climate variables predict bee functional trait variation. (a) Pilosity and (b) lightness both increase with the maximum temperature of the hottest month (ANOVA: $p_{\text{pilosity}} < 0.001$; $\beta_{\text{pilosity}} = 0.577$; $p_{\text{lightness}} < 0.001$; $\beta_{\text{lightness}} = 0.045$). (c) Bee lightness decreases with annual precipitation (ANOVA: $p_{\text{lightness}} = 0.007$; $\beta_{\text{lightness}} = -0.013$). For clarity, trendlines show linear regressions between traits and single environmental variables.

lighter (i.e. higher reflectance) coloration is advantageous for ectotherms in hotter environments because it reduces radiative heat gain and the risk of overheating (Bishop et al., 2016; Bogert, 1949; Clusella Trullas et al., 2007; Kang et al., 2021; Munjal et al., 1997; Watt, 1968).

Additionally, we found that lightness (but not hair coverage) decreased with annual precipitation, in line with Gloger's Rule, which predicts that darker individuals inhabit wetter environments (Delhey, 2019; Gloger, 1833; Rensch, 1929). This rule has been observed in some insects (Lopez et al., 2021; Nishikawa et al., 2010; O'Neill et al., 2017; Williams, 2007), but the underlying mechanisms are contentious, owing to the diverse functions of melanin in camouflage, signalling, and pathogen resistance (Cheng et al., 2018; Delhey, 2019). One possibility that is consistent with the thermal melanism hypothesis considers interactions between thermal and hygric stressors: in hot regions, darker individuals may be favoured in wetter, more vegetated environments that offer refuge from solar radiation and reduced desiccation stress (Delhey, 2019; Xing et al., 2016).

Correspondingly, we found significant biogeographic variation in these traits. Deserts and xeric shrublands hosted hairier, lighter-coloured bees than other biomes sampled, including tropical and subtropical forests, temperate forests, and grasslands and shrublands. Bee taxonomists have long remarked on the prevalence of hair-covered bees in deserts and xeric regions (Michener, 2007). In hot, xeric habitats, hair coverage and resulting light coloration may enhance performance by expanding activity windows and reducing thermal stress (Barrett & O'Donnell, 2023; Shi et al., 2015). Examples of pubescent phenotypes in desert organisms from across the plant and animal kingdoms suggest convergent evolution of hair as an adaptation to heat and aridity (Hadley, 1972; Moles et al., 2020). Bees likely originated in warm, xeric regions 120 Mya (Almeida et al., 2023), and today bee diversity and species richness are greatest in climatically similar habitats (Michener, 1979, 2007). Adaptive variation in these traits may have facilitated the diversification and dispersal of bees to occupy all major terrestrial biomes.

Both pilosity and lightness serve multiple functions in bees, complicating climate relationships to trait variation. Hair serves physiological and ecological functions in bees, functioning in thermoregulation and as the primary vehicle for pollen transport (Heinrich, 1974; Thorp, 2000). The density, structure, and location of specialized pollen-collecting hairs (scopae) vary widely across bee taxa and mediate the uptake of pollen and the efficiency of pollination (Phillips et al., 2018; Thorp, 2000; Woodcock et al., 2019). The extent to which the thermal consequences of hair coverage trade off with its effectiveness in pollen transport is an intriguing avenue for future study. Lightness likewise serves adaptive functions beyond thermoregulation, influencing camouflage, signalling, and immunity (Hines et al., 2022; Stuart-Fox et al., 2017). Indeed, because visible colour is under competing selection for multiple ecological functions, other components of colour outside of the visible spectrum (especially near-infrared, NIR) may vary more consistently with climate (Munro et al., 2019; Wang et al., 2021). Our model quantifies lightness in the visible light spectrum, and so does not account for these other components of solar reflectance. Nevertheless, we find that climate is predictive of visible coloration (Bishop et al., 2016; Kang et al., 2021). Quantifying NIR reflectance across bee taxa may yet reveal even stronger associations to climate variation, and techniques to capture NIR and UV reflectance in images (Munro et al., 2019) enable these data to be analysed with our computer vision workflow.

Importantly, pilosity is a complex and multi-dimensional trait, with hair varying independently in structure, length, density, and spatial distribution across the body, even within an individual (Hines et al., 2022; Pasteels & Pasteels, 1971; Portman et al., 2019). This complexity may account for the appearance of conflicting patterns

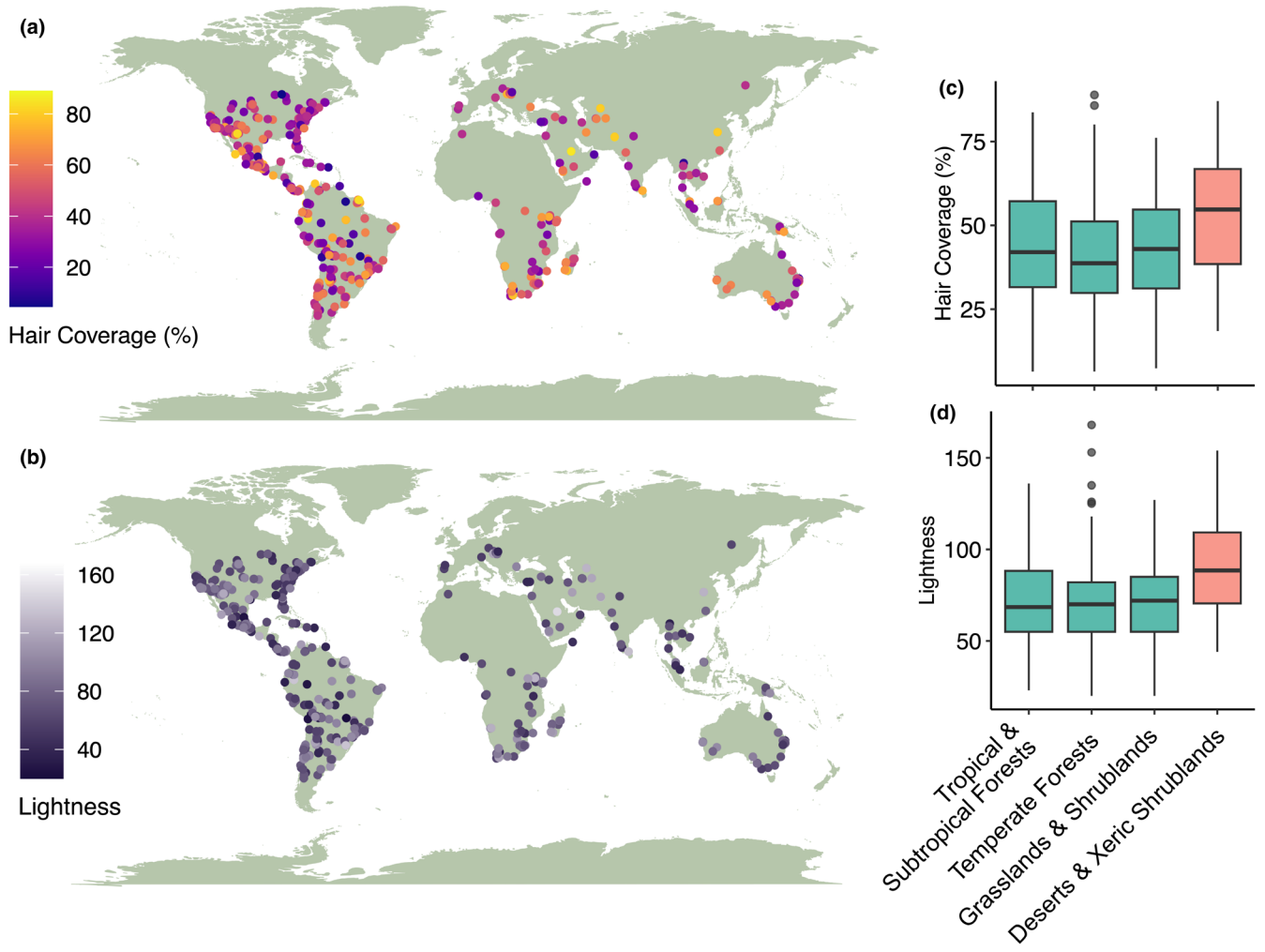

FIGURE 4 Biogeographic variation in bee (a) pilosity and (b) lightness. Both (c) pilosity and (d) lightness are significantly higher in deserts and xeric shrublands than they are in other sampled biomes (estimated marginal means: $p < 0.01$ for all comparisons to desert; $p > 0.05$ for all other comparisons). Colour differences in the boxplot indicate significant differences.

in pilosity variation across studies. Previous work at smaller ecological scales associated hair length with cooler climates (Gonzalez et al., 2022; Osorio-Canadas et al., 2022; Peat et al., 2005; Peters et al., 2016), in line with the insulative function of hair (Casey & Hegel, 1981; Kevan et al., 1982). Hair length is the predominant metric for pilosity in bees, owing largely to its ease of measurement and standardization (Roquer-Beni et al., 2020). However, this method may not scale appropriately to interspecific comparisons of taxonomically diverse bees with variable hair morphologies. Where hair length may reflect the degree of insulation across uniformly hairy body regions, total hair coverage reflects the extent of the hair boundary layer and the exposure of cuticle. Our application of computer vision enabled us to quantify hair coverage, an understudied but functionally significant axis of pilosity, which we found to vary considerably (nearly 20-fold) across bee species. Alternatively, hair coverage may also be an important adaptation to extreme cold habitats, which were underrepresented in our sample. Second, we quantified interspecific trait variation, though both hair and lightness can also vary within species, often in relation to local climate (LaBerge, 1956; Peat et al., 2005). Future work should clarify the extent to which climate drives intraspecific variation in these traits.

Our study demonstrates the promise of computer vision for advancing functional ecological research, as well as the use of biodiversity collections to address current ecological and evolutionary questions. Increasingly, functional traits are being leveraged as a tractable framework for predicting broad patterns in ecology, based on the premise that traits represent easily-quantifiable yet functionally significant organismal characteristics (Gagic et al., 2015; Laughlin et al., 2020; MacLean & Beissinger, 2017; Mcgill et al., 2006; Violle et al., 2007). Nevertheless, many of the traits most relevant to organismal performance, such as those involved in thermoregulation, elude straightforward manual measurement. By automating complex trait measurement tasks, computer vision relieves this quantification bottleneck (Høye et al., 2021; Lürig et al., 2021; Weinstein, 2018), with the additional benefit that these techniques can be replicable and scalable across large datasets, extending the ecological scales at which we can test trait-related hypotheses. Indeed, measurement inconsistency is cited as one reason why climate tends to have poor predictive power in

FIGURE 5 (Legend on next page)

FIGURE 5 Deserts host hairier, lighter-coloured bees than other biomes. Randomly selected subsets of our image dataset, representing bees from deserts and xeric shrublands (top) and from all other sampled biomes (temperate forests, tropical and subtropical forests, grasslands and shrublands; bottom).

large-scale trait meta-analyses (Anderegg, 2023). The impact of these tools will only grow alongside the proliferation of image datasets, particularly specimen images arising from museum collection digitization efforts (Hedrick et al., 2020; Seltmann et al., 2021).

These findings implicate climate as a major selective force in bee trait evolution. Our results provide support for two major ecogeographical rules (the thermal melanism hypothesis and Gloger's Rule), and highlight the interaction between traits as an important determinant of bee biogeography. More broadly, uncovering the climate rules shaping trait evolution will have important implications for predicting the performance and distributions of organisms under future climate scenarios.

AUTHOR CONTRIBUTIONS

Madeleine M. Ostwald, Victor H. Gonzalez, and Katja C. Seltmann conceived the study and supervised the research team. All authors contributed to data collection, model design, data analysis, and manuscript review. Madeleine M. Ostwald wrote the manuscript and conducted the trait analysis.

ACKNOWLEDGEMENTS

We gratefully acknowledge Taite Jimerson, Nathalie Bonnet, Elise Phan, Lauren De Moor, Quinn Dodd-Spiegelberg, Amy Zhao, Alec Buetow, Harper Klauke, Jonathan Wong-Lau, Harleen Kaur, and Joshua Bang for their work creating masks for the training datasets. We also thank Maddie Mohler, Kate Geenan, Natalie Herbison, Colleen Smith, Wyatt Zabinski, and Tianrou You for their work photographing specimens, and Ryan Tang, Elise Phan, and Neha Reddy for their work compiling image data and metadata. We thank JT Miller and Arthur Porto (University of Florida) for valuable feedback and ideas. Finally, we thank two anonymous reviewers whose feedback greatly improved the manuscript. This work was supported by a National Science Foundation (NSF) award (DBI-2102006, DBI-2101851: Extending Anthophila research through image and trait digitization (Big-Bee)) to K.C.S. and V.H.G.

CONFLICT OF INTEREST STATEMENT

The authors declare that they have no competing interests.

DATA AVAILABILITY STATEMENT

All data, code, and images used in these analyses are available through the Zenodo Digital Repositories at https://doi.org/10.5281/zenodo.12572898 and https://zenodo.org/doi/10.5281/zenodo.12572908 (Ostwald et al. 2024).

ORCID

Madeleine M. Ostwald https://orcid.org/0000-0002-9869-8835
Victor H. Gonzalez https://orcid.org/0000-0002-4146-1634
Katja C. Seltmann https://orcid.org/0000-0001-5354-6048

REFERENCES

Almeida, E. A. B., Bossert, S., Danforth, B. N., Porto, D. S., Freitas, F. V., Davis, C. C., Murray, E. A., Blaimer, B. B., Spasojevic, T., Ströher, P. R., Orr, M. C., Packer, L., Brady, S. G., Kuhlmann, M., Branstetter, M. G., & Pie, M. R. (2023). The evolutionary history of bees in time and space. *Current Biology*, *33*, 3409–3422.e6.

Anderegg, L. D. L. (2023). Why can't we predict traits from the environment? *The New Phytologist*, *237*, 1998–2004.

Angilletta, M. J. (2009). *Thermal adaptation: A theoretical and empirical synthesis*. Oxford University Press.

Barrett, M., & O'Donnell, S. (2023). Individual reflectance of solar radiation confers a thermoregulatory benefit to dimorphic males bees (*Centris pallida*) using distinct microclimates. *PLoS One*, *18*(3), e0271250. https://doi.org/10.1371/journal.pone.0271250

Bates, D., Maechler, M., Bolker, B., & Walker, S. (2015). Fitting linear mixed-effects models using lme4. *Journal of Statistical Software*, *67*(1), 1–48. https://doi.org/10.18637/jss.v067.i01

Bishop, T. R., Robertson, M. P., Gibb, H., van Rensburg, B. J., Braschler, B., Chown, S. L., Foord, S. H., Munyai, T. C., Okey, I., Tshivhandekano, P. G., Werenkraut, V., & Parr, C. L. (2016). Ant assemblages have darker and larger members in cold environments. *Global Ecology and Biogeography*, *25*, 1489–1499.

Blackburn, T. M., & Gaston, K. J. (1994). Animal body size distributions: Pattems, mechanisms and implications. *Trends in Ecology & Evolution*, *9*, 471–474.

Bogert, C. M. (1949). Thermoregulation in reptiles, a factor in evolution. *Evolution*, *3*(3), 195–211. https://doi.org/10.2307/2405558

Bossert, S., Wood, T. J., Patiny, S., Michez, D., Almeida, E. A. B., Minckley, R. L., Packer, L., Neff, J. L., Copeland, R. S., Straka, J., Pauly, A., Griswold, T., Brady, S. G., Danforth, B. N., & Murray, E. A. (2022). Phylogeny, biogeography and diversification of the mining bee family Andrenidae. *Systematic Entomology*, *47*, 283–302.

Brown, J. (1995). *Macroecology*. University of Chicago Press.

Burrows, S. (2021). Exotic Bee ID.

Buxton, J. T., Robert, K. A., Marshall, A. T., Dutka, T. L., & Gibb, H. (2021). A cross-species test of the function of cuticular traits in ants (Hymenoptera: Formicidae). *Myrmecol. News*, *31*, 31–46.

Casey, T., & Hegel, J. (1981). Caterpillar setae: Insulation for an ectotherm. *Science*, *214*(4525), 1131–1133. https://doi.org/10.1126/science.214.4525.1131

Cheng, W., Xing, S., Chen, Y., Lin, R., Bonebrake, T. C., & Nakamura, A. (2018). Dark butterflies camouflaged from predation in dark tropical forest understories. *Ecological Entomology*, *43*, 304–309.

Chown, S. L., & Gaston, K. J. (2010). Body size variation in insects: A macroecological perspective. *Biological Reviews*, *85*, 139–169.

Church, N. S. (1960). Heat loss and the body temperatures of flying insects. II. Heat conduction within the body and its loss by radiation and convection. *Journal of Experimental Biology*, *37*, 186–212.

Clusella Trullas, S., Van Wyk, J. H., & Spotila, J. R. (2007). Thermal melanism in ectotherms. *Journal of Thermal Biology*, *32*, 235–245.

da Silva, C. R. B., Beaman, J. E., Youngblood, J. P., Kellermann, V., & Diamond, S. E. (2023). Vulnerability to climate change increases with trophic level in terrestrial organisms. *Science of the Total Environment*, *865*, 161049.

De Boer, P.-T., Kroese, D. P., Mannor, S., & Rubinstein, R. Y. (2005). A tutorial on the cross-entropy method. *Annals of Operations Research*, *134*, 19–67.

Delhey, K. (2019). A review of Gloger's rule, an ecogeographical rule of colour: Definitions, interpretations and evidence. *Biological Reviews*, *94*, 1294–1316.

Ehleringer, J., Björkman, O., & Mooney, H. A. (1976). Leaf pubescence: Effects on absorptance and photosynthesis in a desert shrub. *Science*, *192*, 376–377.

Fick, S., & Hijmans, R. (2017). WorldClim 2: New 1 km spatial resolution climate surfaces for global land areas. *International Journal of Climatology*, *37*, 4302–4315.

Freitas, F. V., Branstetter, M. G., Franceschini-Santos, V. H., Dorchin, A., Wright, K. W., López-Uribe, M. M., Griswold, T., Silveira, F. A., & Almeida, E. A. B. (2023). UCE phylogenomics, biogeography, and classification of long-horned bees (Hymenoptera: Apidae: Eucerini), with insights on using specimens with extremely degraded DNA. *Insect Systematics and Diversity*, *7*, 3.

Gagic, V., Bartomeus, I., Jonsson, T., Taylor, A., Winqvist, C., Fischer, C., Slade, E. M., Steffan-Dewenter, I., Emmerson, M., Potts, S. G., Tscharntke, T., Weisser, W., & Bommarco, R. (2015). Functional identity and diversity of animals predict ecosystem functioning better than species-based indices. *Proceedings of the Royal Society B: Biological Sciences*, *282*, 20142620.

Gaston, K. J., Chown, S. L., & Evans, K. L. (2008). Ecogeographical rules: Elements of a synthesis. *Journal of Biogeography*, *35*, 483–500.

Gharaee, Z., Lowe, S. C., Gong, Z. M., Arias, P. M., Pellegrino, N., Wang, A. T., Haurum, J. B., Zarubiieva, I., Kari, L., Steinke, D., Taylor, G. W., Fieguth, P., & Chang, A. X. (2025). BIOSCAN-5M: A Multimodal Dataset for Insect Biodiversity. http://arxiv.org/abs/2406.12723

Gloger, C. (1833). *Das Abändern der Vögel durch Einfluss des Klima's*. August Schulz & Co.

Gonçalves, R. B. (2016). A molecular and morphological phylogeny of the extant Augochlorini (Hymenoptera, Apoidea) with comments on implications for biogeography. *Systematic Entomology*, *41*, 430–440.

Gonzalez, V. H., Griswold, T., Praz, C. J., & Danforth, B. N. (2012). Phylogeny of the bee family Megachilidae (Hymenoptera: Apoidea) based on adult morphology. *Systematic Entomology*, *37*, 261–286.

Gonzalez, V. H., Gustafson, G. T., & Engel, M. S. (2019). Morphological phylogeny of Megachilini and the evolution of leaf-cutter behavior in bees (Hymenoptera: Megachilidae): Evolution of leaf-cutter behavior in bees. *Journal of Melittology*, *85*, 1–123. https://doi.org/10.17161/jom.v0i85.11541

Gonzalez, V. H., Oyen, K., Vitale, N., & Ospina, R. (2022). Neotropical stingless bees display a strong response in cold tolerance with changes in elevation. *Conservation Physiology*, *10*, coac073.

Gonzalez, V. H., Smith-Pardo, A. H., & Engel, M. S. (2017). Phylogenetic relationships of a new genus of Calliopsine bees from Peru, with a review of *Spinoliella* Ashmead (Hymenoptera: Andrenidae). *Bulletin of the American Museum of Natural History*, *412*, 1–71. https://doi.org/10.1206/0003-0090-412.1.1

Guangchuang, Y., Smith, D., Zhu, H., Guan, Y., & Lam, T. T.-Y. (2017). ggtree: An R package for visualization and annotation of phylogenetic trees with their covariates and other associated data. *Methods in Ecology and Evolution*, *8*(1), 28–36. https://doi.org/10.1111/2041-210X.12628

Hadley, N. (1972). Desert species and adaptation: Plants and animals in arid environments show many striking similarities in their morphological and physiological adaptations. *American Scientist*, *60*, 338–347.

Hadley, N. (1994). *Water relations of terrestrial arthropods*. Academic Press.

He, J., Tu, J., Yu, J., & Jiang, H. (2023). A global assessment of Bergmann's rule in mammals and birds. *Global Change Biology*, *29*(18), 5199–5210. https://doi.org/10.1111/gcb.16860

Hedrick, B. P., Heberling, J. M., Meineke, E. K., Turner, K. G., Grassa, C. J., Park, D. S., Kennedy, J., Clarke, J. A., Cook, J. A., Blackburn, D. C., Edwards, S. V., & Davis, C. C. (2020). Digitization and the future of natural history collections. *Bioscience*, *70*, 243–251.

Heinrich, B. (1974). Thermoregulation in endothermic insects. *Science*, *185*, 747–756.

Henríquez-Piskulich, P., Hugall, A. F., & Stuart-Fox, D. (2024). A supermatrix phylogeny of the world's bees (Hymenoptera: Anthophila). *Molecular Phylogenetics and Evolution*, *190*, 107963.

Hijmans, R. J. (2023). raster: Geographic data analysis and modeling.

Hines, H. M., Kilpatrick, S. K., Mikó, I., Snellings, D., López-Uribe, M. M., & Tian, L. (2022). The diversity, evolution, and development of setal morphologies in bumble bees (Hymenoptera: Apidae: *Bombus* spp.). *PeerJ*, *10*, e14555.

Høye, T. T., Ärje, J., Bjerge, K., Hansen, O. L. P., Iosifidis, A., Leese, F., Mann, H. M. R., Meissner, K., Melvad, C., & Raitoharju, J. (2021). Deep learning and computer vision will transform entomology. *Proceedings of the National Academy of Sciences of the United States of America*, *118*, e2002545117.

Huang, H., Lin, L., Tong, R., Hu, H., Zhang, Q., Iwamoto, Y., Han, X., Chen, Y.-W., & Wu, J. (2020). UNet 3+: A full-scale connected UNet for medical image segmentation. In *ICASSP 2020–2020 IEEE International Conference on Acoustics, Speech and Signal Processing (ICASSP)* (pp. 1055–1059). IEEE.

Iglovikov, V., & Shvets, A. (2018). TernausNet: U-Net with VGG11 encoder pre-trained on imagenet for image segmentation. [Preprint]. http://arxiv.org/abs/1801.05746

Kahle, D., & Wickham, H. (2013). Ggmap: Spatial visualization with ggplot2. *The R Journal*, *5*, 144–161.

Kang, C., Im, S., Lee, W. Y., Choi, Y., Stuart-Fox, D., & Huertas, B. (2021). Climate predicts both visible and near-infrared reflectance in butterflies. *Ecology Letters*, *24*, 1869–1879.

Kellermann, V., Hoffmann, A. A., Overgaard, J., Loeschcke, V., & Sgro, C. M. (2018). Plasticity for desiccation tolerance across Drosophila species is affected by phylogeny and climate in complex ways. *Proceedings of the Royal Society B: Biological Sciences*, *285*, 20180048.

Kevan, P. G., Jensen, T. S., & Shorthouse, J. D. (1982). Body temperature and behavioral thermoregulation of high arctic woolly-bear caterpillars and pupae (*Gynaephora rossii*, Lymantriidae: Lepidoptera) and the importance of sunshine. *Arctic, Antarctic, and Alpine Research*, *14*, 125–136.

Kingma, D. P., & Ba, J. (2017). Adam: A method for stochastic optimization. [Preprint]. http://arxiv.org/abs/1412.6980

LaBerge, W. E. (1956). A revision of the bees of the genus *Melissodes* in north and Central America. Part I. (Hymenoptera, Apidae). *University of Kansas Science Bulletin*, *37*(18), 911–1194. https://doi.org/10.5962/bhl.part.24549

Laughlin, D. C., Gremer, J. R., Adler, P. B., Mitchell, R. M., & Moore, M. M. (2020). The net effect of functional traits on fitness. *Trends in Ecology & Evolution*, *35*, 1037–1047.

Lenoir, J., Bertrand, R., Comte, L., Bourgeaud, L., Hattab, T., Murienne, J., & Grenouillet, G. (2020). Species better track climate warming in the oceans than on land. *Nature Ecology & Evolution*, *4*, 1044–1059.

Lenth, R. (2021). emmeans: Estimated marginal means, aka least-squares means.

Litman, J. R., Praz, C. J., Danforth, B., Griswold, T. L., & Cardinal, S. (2013). Origins, evolution, and diversification of Cleptoparasitic lineages in long-tongued bees. *Evolution*, *67*, 2982–2998.

Lopez, V. M., Azevedo Tosta, T. A., da Silva, G. G., Bartholomay, P. R., Williams, K. A., & Guillermo-Ferreira, R. (2021). Color lightness of velvet ants (Hymenoptera: Mutillidae) follows an environmental gradient. *Journal of Thermal Biology*, *100*, 103030.

Lürig, M. D., Donoughe, S., Svensson, E. I., Porto, A., & Tsuboi, M. (2021). Computer vision, machine learning, and the promise of Phenomics in ecology and evolutionary biology. *Frontiers in Ecology and Evolution*, *9*, 642774. https://doi.org/10.3389/fevo.2021.642774

MacArthur, R. H. (1972). *Geographical ecology: Patterns in the distribution of species*. Princeton University Press.

MacLean, S., & Beissinger, S. R. (2017). Species' traits as predictors of range shifts under contemporary climate change: A review and

meta-analysis. *Global Change Biology*, *23*(10), 4094–4105. https://doi.org/10.1111/gcb.13736

Mcgill, B., Enquist, B., Weiher, E., & Westoby, M. (2006). Rebuilding community ecology from functional traits. *Trends in Ecology & Evolution*, *21*, 178–185.

Mershon, J., Becker, M., & Bickford, C. (2015). Linkage between trichome morphology and leaf optical properties in New Zealand alpine *Pachycladon* (Brassicaceae). *New Zealand Journal of Botany*, *53*(3), 175–182. https://doi.org/10.1080/0028825X.2015.1042486

Michener, C. (1979). Biogeography of the bees. *Annals of the Missouri Botanical Garden*, *66*(3), 277. https://doi.org/10.2307/2398833

Michener, C. (2007). *The bees of the world*. Johns Hopkins University Press.

Michez, D., Patiny, S., & Danforth, B. N. (2009). Phylogeny of the bee family Melittidae (Hymenoptera: Anthophila) based on combined molecular and morphological data. *Systematic Entomology*, *34*, 574–597.

Moles, A. T., Laffan, S. W., Keighery, M., Dalrymple, R. L., Tindall, M. L., & Chen, S. C. (2020). A hairy situation: Plant species in warm, sunny places are more likely to have pubescent leaves. *Journal of Biogeography*, *47*, 1934–1944.

Munjal, A., Karan, D., Gibert, P., Moreteau, B., Parkash, R., & David, J. R. (1997). Thoracic trident pigmentation in Drosophila melanogaster: Latitudinal and altitudinal clines in Indian populations. *Genetics, Selection, Evolution*, *29*, 601.

Munro, J. T., Medina, I., Walker, K., Moussalli, A., Kearney, M. R., Dyer, A. G., Garcia, J., Rankin, K. J., & Stuart-Fox, D. (2019). Climate is a strong predictor of near-infrared reflectance but a poor predictor of colour in butterflies. *Proceedings of the Royal Society B: Biological Sciences*, *286*, 20190234.

Nishikawa, M., Ikeda, H., Kubota, K., & Sota, T. (2010). Taxonomic redefinition and natural history of the endemic silphid beetle *Silpha longicornis* (Coleoptera: Silphidae) of Japan, with an analysis of its geographic variation. *Zootaxa*, *2648*(1), 1–31. https://doi.org/10.11646/zootaxa.2648.1.1

Ollerton, J., Winfree, R., & Tarrant, S. (2011). How many flowering plants are pollinated by animals? *Oikos*, *120*, 321–326.

Olson, D. M., Dinerstein, E., Wikramanayake, E. D., Burgess, N. D., Powell, G. V. N., Underwood, E. C., D'amico, J. A., Itoua, I., Strand, H. E., Morrison, J. C., Loucks, C. J., Allnutt, T. F., Ricketts, T. H., Kura, Y., Lamoreux, J. F., Wettengel, W. W., Hedao, P., & Kassem, K. R. (2001). Terrestrial ecoregions of the world: A new map of life on earth. *Bioscience*, *51*, 933.

O'Neill, E. M., Hearn, E. J., Cogbill, J. M., & Kajita, Y. (2017). Rapid evolution of a divergent ecogeographic cline in introduced lady beetles. *Evolutionary Ecology*, *31*(5), 695–705. https://doi.org/10.1007/s10682-017-9908-1

Osorio-Canadas, S., Flores-Hernández, N., Sánchez-Ortiz, T., & Valiente-Banuet, A. (2022). Changes in bee functional traits at community and intraspecific levels along an elevational gradient in a Mexical-type scrubland. *Oecologia*, *200*, 145–158.

Ostwald, M., Chen, K., Alexander, N., Ding, L., Gonzalez, V., & Seltmann, K. C. (2024). Data for: Climate explains global functional trait variation in bees. *Zenodo*. https://doi.org/10.5281/zenodo.12572898

Ostwald, M., Gonzalez, V. H., Chang, C., Vitale, N., Lucia, M., & Seltmann, K. C. (2023). Toward a functional trait approach to bee ecology. Authorea Preprints.

Paradis, E., & Schliep, K. (2019). Ape 5.0: An environment for modern phylogenetics and evolutionary analyses in R. *Bioinformatics*, *35*(3), 526–528. https://doi.org/10.1093/bioinformatics/bty633

Pasteels, J., & Pasteels, J. (1971). Etude au microscope électronique à balayage des plages glandulaires tergales chez des espèces du genre Megachile (Hymenoptera, Apoïda, Megachilidae). Comptes Rendus de L'académie Des Sciences-Series IV-Physics, Astrophysics.

Peat, J., Darvill, B., Ellis, J., & Goulson, D. (2005). Effects of climate on intra- and interspecific size variation in bumble-bees. *Functional Ecology*, *19*, 145–151.

Peters, M. K., Peisker, J., Steffan-Dewenter, I., & Hoiss, B. (2016). Morphological traits are linked to the cold performance and distribution of bees along elevational gradients. *Journal of Biogeography*, *43*, 2040–2049.

Phillips, B. B., Williams, A., Osborne, J. L., & Shaw, R. F. (2018). Shared traits make flies and bees effective pollinators of oilseed rape (*Brassica napus* L.). *Basic and Applied Ecology*, *32*, 66–76.

Pisanty, G., Richter, R., Martin, T., Dettman, J., & Cardinal, S. (2022). Molecular phylogeny, historical biogeography and revised classification of andrenine bees (Hymenoptera: Andrenidae). *Molecular Phylogenetics and Evolution*, *170*, 107151.

Portman, Z. M., Orr, M. C., & Griswold, T. (2019). A review and updated classification of pollen gathering behavior in bees (Hymenoptera, Apoidea). *Journal of Hymenoptera Research*, *71*, 171–208.

R Core Team. (2024). *R: A language and environment for statistical computing*. R Foundation for Statistical Computing.

Rasmussen, C., & Cameron, S. A. (2009). Global stingless bee phylogeny supports ancient divergence, vicariance, and long distance dispersal: STINGLESS BEE PHYLOGENY. *Biological Journal of the Linnean Society*, *99*(1), 206–232. https://doi.org/10.1111/j.1095-8312.2009.01341.x

Rensch, B. (1929). *Das Prinzip geographischer Rassenkreise und das Problem der Artbildung*. Gebrueder Borntraeger.

Revell, L. J. (2024). phytools 2.0: An updated R ecosystem for phylogenetic comparative methods (and other things). *PeerJ*, *12*, e16505.

Rogerson, P. A. (2001). *Statistical methods for geography*. Sage.

Ronneberger, O., Fischer, P., & Brox, T. (2015). U-Net: Convolutional networks for biomedical image segmentation. [Preprint]. http://arxiv.org/abs/1505.04597

Roquer-Beni, L., Rodrigo, A., Arnan, X., Klein, A. M., Fornoff, F., Boreux, V., & Bosch, J. (2020). A novel method to measure hairiness in bees and other insect pollinators. *Ecology and Evolution*, *10*, 2979–2990.

Seltmann, K., Allen, J., Brown, B., Carper, A., Engel, M., Franz, N., Gilbert, E., Grinter, C., Gonzalez, V., Horsley, P., Lee, S., Maier, C., Miko, I., Morris, P., Oboyski, P., Pierce, N., Poelen, J., Scott, V., Smith, M., … Tucker, E. (2021). Announcing big-bee: An initiative to promote understanding of bees through image and trait digitization. *Biodiversity Information Science and Standards*, *5*, e74037.

Shi, N. N., Tsai, C. C., Camino, F., Bernard, G. D., Yu, N., & Wehner, R. (2015). Keeping cool: Enhanced optical reflection and radiative heat dissipation in Saharan silver ants. *Science*, *349*, 298–301.

Skelton, R. P., Midgley, J. J., Nyaga, J. M., Johnson, S. D., & Cramer, M. D. (2012). Is leaf pubescence of Cape Proteaceae a xeromorphic or radiation-protective trait? *Australian Journal of Botany*, *60*(2), 104–113. https://doi.org/10.1071/BT11231

Stuart-Fox, D., Newton, E., & Clusella-Trullas, S. (2017). Thermal consequences of colour and near-infrared reflectance. *Philosophical Transactions of the Royal Society of London. Series B, Biological Sciences*, *372*(1724), 20160345. https://doi.org/10.1098/rstb.2016.0345

Sunday, J. M., Bates, A. E., & Dulvy, N. K. (2011). Global analysis of thermal tolerance and latitude in ectotherms. *Proceedings of the Royal Society B: Biological Sciences*, *278*, 1823–1830.

Thorp, R. W. (2000). The collection of pollen by bees. *Plant Systematics and Evolution*, *222*, 211–223.

USGS Interagency Bee Lab, Droege, S. (2010). USGS Native Bee Inventory and Monitoring Program Images. Flickr. https://www.flickr.com/photos/usgsbiml/albums/.

Van Horn, G., Aodha, O. M., Song, Y., Cui, Y., Sun, C., Shepard, A., Adam, H., Perona, P., & Belongie, S. (2018). The iNaturalist Species Classification and Detection Dataset. [Preprint]. http://arxiv.org/abs/1707.06642

Violle, C., Navas, M. L., Vile, D., Kazakou, E., Fortunel, C., Hummel, I., & Garnier, E. (2007). Let the concept of trait be functional! *Oikos*, *116*, 882–892.

Violle, C., Reich, P. B., Pacala, S. W., Enquist, B. J., & Kattge, J. (2014). The emergence and promise of functional biogeography. *Proceedings of the National Academy of Sciences of the United States of America*, *111*, 13690–13696.

Wang, L.-Y., Franklin, A. M., Black, J. R., & Stuart-Fox, D. (2021). Heating rates are more strongly influenced by near-infrared than visible reflectance in beetles. *Journal of Experimental Biology*, *224*(19), jeb242898. https://doi.org/10.1242/jeb.242898

Watt, W. B. (1968). Adaptive significance of pigment polymorphisms in Colias butterflies. I. Variation of melanin pigment in relation to thermoregulation. *Evolution*, *22*, 437–458.

Weinstein, B. G. (2018). A computer vision for animal ecology. *The Journal of Animal Ecology*, *87*, 533–545.

Whittaker, R. J., Willis, K. J., & Field, R. (2001). Scale and species richness: Towards a general, hierarchical theory of species diversity. *Journal of Biogeography*, *28*, 453–470.

Williams, P. (2007). The distribution of bumblebee colour patterns worldwide: Possible significance for thermoregulation, crypsis, and warning mimicry. *Biological Journal of the Linnean Society*, *92*, 97–118.

Woodcock, B. A., Garratt, M. P. D., Powney, G. D., Shaw, R. F., Osborne, J. L., Soroka, J., Lindström, S. A. M., Stanley, D., Ouvrard, P., Edwards, M. E., Jauker, F., McCracken, M. E., Zou, Y., Potts, S. G., Rundlöf, M., Noriega, J. A., Greenop, A., Smith, H. G., Bommarco, R., … Pywell, R. F. (2019). Meta-analysis reveals that pollinator functional diversity and abundance enhance crop pollination and yield. *Nature Communications*, *10*, 1481.

Xing, S., Bonebrake, T. C., Tang, C. C., Pickett, E. J., Cheng, W., Greenspan, S. E., Williams, S. E., & Scheffers, B. R. (2016). Cool habitats support darker and bigger butterflies in Australian tropical forests. *Ecology and Evolution*, *6*, 8062–8074.

How to cite this article: Ostwald, M. M., Chen, K., Alexander, N., Ding, L., Gonzalez, V. H., & Seltmann, K. C. (2025). Climate explains global functional trait variation in bees. *Functional Ecology*, *39*, 1748–1760. https://doi.org/10.1111/1365-2435.70051